

# The Exceptional Aspects of the Confined X-class Flares of Solar Active Region 2192

Julia K. Thalmann<sup>1</sup>, Yang Su<sup>1,2</sup>, Manuela Temmer<sup>1</sup>  
 and  
 Astrid M. Veronig<sup>1</sup>

<sup>1</sup>Institute of Physics/IGAM, University of Graz,  
 Universitätsplatz 5/II, 8010 Graz, Austria  
 email: julia.thalmann@uni-graz.at

<sup>2</sup>Key Laboratory of Dark Matter & Space Astronomy,  
 Purple Mountain Observatory, Chinese Academy of Sciences,  
 2 West Beijing Road, 210008 Nanjing, China  
 email: yang.su@pmo.ac.cn

**Abstract.** During late October 2014, active region NOAA 2192 caused an unusual high level of solar activity, within an otherwise weak solar cycle. While crossing the solar disk, during a period of 11 days, it was the source of 114 flares of *GOES* class C1.0 and larger, including 29 M- and 6 X-flares. Surprisingly, none of the major flares (*GOES* class M5.0 and larger) was accompanied by a coronal mass ejection, contrary to statistical tendencies found in the past. From modeling the coronal magnetic field of NOAA 2192 and its surrounding, we suspect that the cause of the confined character of the flares is the strong surrounding and overlying large-scale magnetic field. Furthermore, we find evidence for multiple magnetic reconnection processes within a single flare, during which electrons were accelerated to unusual high energies.

**Keywords.** Sun: atmosphere, Sun: chromosphere, Sun: corona, Sun: magnetic fields, Sun: flares, Sun: UV radiation, Sun: X-rays, gamma rays, methods: numerical

We analyze the unexpected high solar activity associated to active region NOAA 2192 which hosted more than one hundred flares during disk passage, including 6 *GOES* class X flares (Fig. 1). NOAA 2192 covered a large part of the solar surface (roughly 15–20 times Earth’s diameter in east-west direction; see Fig. 2a) and the intensive flaring activity was rooted in its complex and strong surface magnetic field configuration. It was classified as  $\beta\gamma\delta$ -configuration and hosted umbral field strengths of  $> 2.5$  kG (the latter corresponding to the upper end of known statistics of umbral magnetic field strengths).

The flaring activity of NOAA 2192 was exceptional in that all of the large (*GOES* class  $\geq M5.0$ ) flares were confined, i. e., that no associated ejection of coronal material into interplanetary space was observed. This is special since we know of the affinity of large flares and coronal mass ejections to occur together (see Yashiro et al. 2006). In Thalmann et al. (2015), we analyzed some exceptional aspects of the major flares that originated from NOAA 2192 on October 22 and 24, 2014. In the following, we summarize the most important findings.

## 1. Magnetic reconnection at large heights in the corona

All of the analyzed major flares were obviously similar in morphology (see Fig. 2b–d). The observed flare ribbons showed a large initial separation and no substantial growth of separation at later times (cf. Fig. 1 of Thalmann et al. 2015). That suggests that the reconnection site was situated at large coronal heights ( $\approx 50$  Mm above photospheric levels)

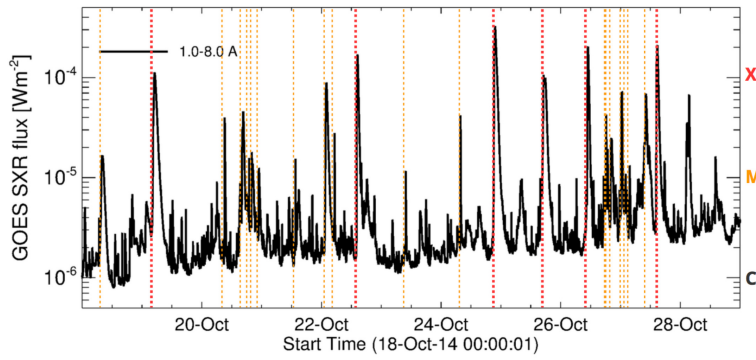


**Figure 1.** *GOES* 1.0–8.0 Å soft X-ray flux between October 18 and 29, 2014. Vertical dashed lines indicate the time when a flare occurred. Yellow and red lines mark the peak time of M- and X-flares, respectively. Only peak times of flares M1.0 and larger are shown. All indicated flares originated from NOAA 2192.

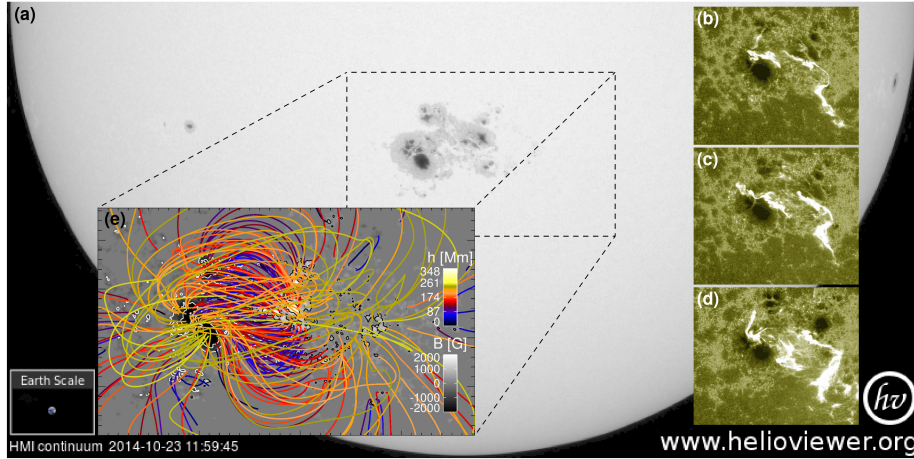


**Figure 2.** (a) *SDO*/HMI white-light continuum image on October 23, 2014 at 12:00 UT, covering the southern hemisphere of the Sun. For an impression of the size of NOAA 2192, Earth’s size is indicated in the lower left corner. Panels (b)–(d) show the *SDO*/AIA 1600 Å emission in the active region center at the peak time of three X-flares, showing a clearly similar morphology. Panel (e): Sample field lines calculated from a nonlinear force-free magnetic field model, colored according to the apex height of each field line. The active region center consists of a system of highly sheared fields (black/blue/purple lines).

during these events. That corresponds roughly to the average pre-flare apex height of the strongly sheared magnetic field structures in the center of the active region, calculated from a nonlinear force-free magnetic field model (see Fig. 2e).

## 2. Multiple magnetic reconnection events during a single flare

Analysis of the flare ribbon emission during the X1.6 flare, peaking on October 22 at 14:28 UT, revealed that the extreme ultraviolet light curves of a number of flare kernels (i.e., the constituents of the typical ribbon-like flare emission) exhibited two distinct peaks. Examples of typical light curves of flare kernels located in the negative and positive polarity region of NOAA 2192 are shown in Fig. 3 (see also Fig. 5 of Thalmann

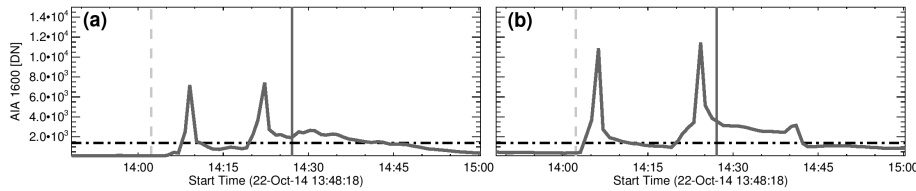


**Figure 3.** *SDO/AIA* 1600 Å light curves, typical for localized kernels within flare ribbons located in the (a) negative and (b) positive polarity domain of NOAA 2192. The vertical dashed/solid lines mark the nominal start and peak time of the X1.6 flare, respectively, based on the *GOES* soft X-ray flux. The horizontal dotted line indicates the intensity threshold used to track flaring pixels.

et al. 2015). Importantly, those peaks occurred co-temporal with two hard X-ray bursts (compare Fig. 3 of Thalmann et al. 2015) and co-spatial with H $\alpha$  flare kernels and non-thermal X-ray sources (cf. Fig. 4 of Thalmann et al. 2015). These findings provide evidence that multiple reconnection events can occur within a single flare, i.e., that the same magnetic field structures can be involved in successive reconnection events. The *RHESSI* hard X-ray data revealed steep non-thermal power-law spectra of the flare-accelerated electrons (cf. Fig. 3b–3e of Thalmann et al. 2015). The total energy in electron derived from the spectra indicated an unusually large amount of total kinetic energy that resided in the accelerated electrons, in contrast to typical (eruptive) flares of class X1.

### 3. External magnetic field constraining the development of mass ejections

Modeling of the large-scale (potential) coronal neighborhood of NOAA 2192, around the X3.1 flare (peak time 21:41 UT on October 24) revealed a north-south oriented magnetic arcade on top of the flaring region (cf. Fig. 2 of Thalmann et al. 2015). We estimated the average strength of the overlying field and its decay index  $n$  with height (i.e., a measure for the decay of the constraining background field; see Fig. 4). We stress that, by definition, these values have to be approximated from a potential (current-free) magnetic field configuration. For values of  $n \gtrsim 1.5$ , theory predicts favorable conditions for the onset of torus instability. Hence, the external field has to decrease sufficiently fast in the direction of the major radius of a torus carrying a toroidal current (Kliem & Török 2006). In the present case, this was found only true for heights of  $\sim 70$  Mm above the solar surface, i.e., at much larger heights than the apexes of the highly sheared core-fields, involved in the flaring process. Also Sun et al. (2015) studied the evolution of NOAA 2191 and pointed out the strength of the overlying field. In addition they found that this CME-less active region revealed a weaker non-potentiality and smaller flare-related magnetic field changes than CME-associated flaring regions.

Note that the concept of torus instability is well defined only for a configuration consisting of a well-defined, narrow current following the axis of a flux tube (the current-carrying torus). The applicability of this concept, to complex magnetic field configurations such as that of NOAA 2192 is not straight forward, however, since it consists of widely spread electric currents. Thus, we also employed a more general measure for the strength of the constraining background field, the flux ratio, in the form  $F_{\text{low}}/F_{\text{high}}$  above the polarity inversion line. Here,  $F_{\text{low}}$  is the average horizontal flux in the height range  $1.0 < h < 1.1 R_{\text{Sun}}$  (covering the sheared core field) and  $F_{\text{high}}$  is the corresponding flux within  $1.1 < h < 1.5 R_{\text{Sun}}$  (covering the overlying arcade that may prevent the underlying core field from erupting). We found  $F_{\text{low}}/F_{\text{high}} \approx 0.3$ , a value even lower than the flux ratios found by Wang & Zhang (2007) for confined X-flares ( $1.0 \lesssim F_{\text{low}}/F_{\text{high}} \lesssim 6.0$ ).

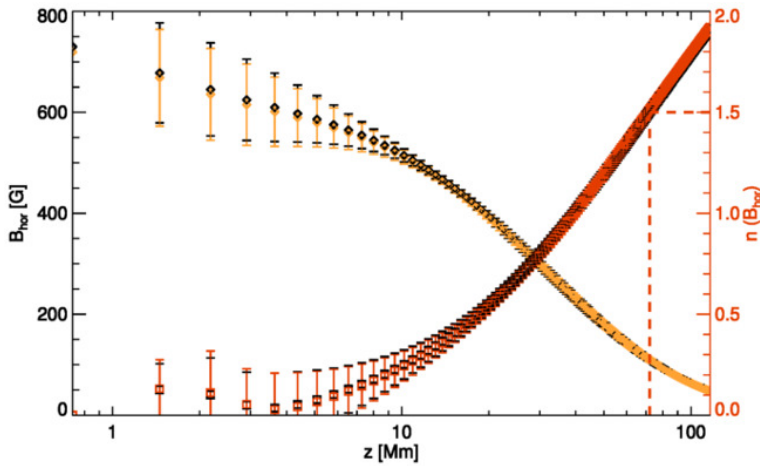


**Figure 4.** Average magnitude of the horizontal magnetic field above the main polarity inversion line of NOAA 2192 prior to and after the X3.1 flare on October 24. Diamonds and squares mark the average horizontal field magnitude,  $B_{\text{hor}}$ , and the decay index  $n$ , respectively. Black symbols refer to the pre-flare and colored symbols to the post-flare magnetic field configuration.

To summarize, we find that the strength of the coronal fields in the neighborhood of active regions may be essential in determining whether or not the upcoming flaring activity is associated to a mass ejection or not. That means that a strong background field may prevent an otherwise unstable flux rope from erupting. Our nonlinear force-free magnetic field modeling, however, did not reveal the presence of a fully emerged, well-defined flux rope, that could be subject to, e.g., torus instability after all. Instead, it shows a system of rather strongly sheared magnetic fields (see Fig. 2e). This is supported by the observation of Veronig & Polanec (2015), who did not find evidence for an existing filament that would indicate the presence of a flux rope in the course of the X1.6 flare on October 22. Therefore, they put forward an emerging-flux scenario as an explanation for the associated large but confined flaring activity.

### Acknowledgements

The authors thankfully acknowledge support from the Austrian Science Fund (FWF): P25383-N27, P27292-N20, and V195-N16.

### References

- Pötzi, W. and Veronig, A. M. and Riegler, G. and Amerstorfer, U. and Pock, T. and Temmer, M. and Polanec, W. and Baumgartner, D. J. 2015, *Sol. Phys.*, 290, 951
- Sun, X. and Bobra, M. G. and Hoeksema, J. T. and Liu, Y. and Li, Y. and Shen, C. and Couvidat, S. and Norton, A. A. and Fisher, G. H. 2015, *ApJ* (Letters), 804, L28
- Thalmann, J. K. and Su, Y. and Temmer, M. and Veronig, A. M. 2015, *ApJ* (Letters), 801, L23
- Török, T. and Kliem, B. 2005, *ApJ* (Letters), 630, L97
- Kliem, B. and Török, T. 2006, *Phys. Rev. (Letters)*, 96, 255002
- Veronig, A. M. and Polanec, W. 2015, *Sol. Phys.*, 290, 2923
- Wang, Y. and Zhang, J. 2007, *ApJ*, 665, 1428
- Yashiro, S. and Akiyama, S. and Gopalswamy, N. and Howard, R. A. 2006, *ApJ* (Letters), 650, L143